

Detailed Chemical Abundances of Extragalactic Globular Clusters

R. A. Bernstein

Astronomy Dept, University of Michigan, 500 Church St., Ann Arbor, MI, 48109

A. McWilliam

Carnegie Observatories, 813 Santa Barbara St., Pasadena, CA, 91101

Abstract.

We outline a method to measure the detailed chemical composition of extragalactic (unresolved) globular clusters (GCs) from echelle spectra of their integrated light. Our goal is to use this method to measure abundance patterns of GCs in distant spiral and elliptical galaxies to constrain their formation histories. To develop this technique we have obtained a “training set” of integrated-light spectra of resolved GCs in the Milky Way and LMC by scanning across the clusters during exposures. Our training set also include spectra of individual stars in those GCs from which abundances can be obtained in the normal way to provide a check on our integrated-light results. We present here the preliminary integrated-light analysis of one GC in our training set, NGC 104 (47 Tuc), and outline some of the techniques utilized and problems encountered in that analysis.

1. Introduction

We are developing a method which will let us measure detailed chemical abundances of Globular Clusters (GCs) from high-resolution, echelle spectra of their integrated light. Our goal is to use the detailed abundance patterns of GC systems in galaxies as distant as 4–5 Mpc to constrain their formation and chemical enrichment histories in the same way as the abundance patterns of old stars have been used to do so in the Milky Way (*e.g.* Edvardsson *et al.* 1993; McWilliam *et al.* 1995; Prochaska *et al.* 2003; Bensby *et al.* 2004ab; Fulbright, McWilliam & Rich 2005).

The elements which are the most useful for understanding the processes of galaxy evolution are those which are returned to the ISM primarily through either high-mass, core-collapse SNe (Type II = SNII) or through low-mass, accretion-induced SNe (Type Ia = SNIa). The key is that the former (SNII) evolve on time-scales of order 10^6 years, while the latter (SNIa) generally take of order 10^9 years. Elements produced by SNII — “ α -elements” (*e.g.* Si, S, Ca) and r-process elements (*e.g.* Eu) — will therefore build up rapidly over the first few megayears of star formation or in a starburst. Elements produced in SNIa and SNII — Fe and Fe-peak elements (*e.g.* Sc, V, Cr, Mn, Fe, Co, Ni) — build up over many gigayears as the contribution from SNIa increases. The ratio $[\alpha/\text{Fe}]$

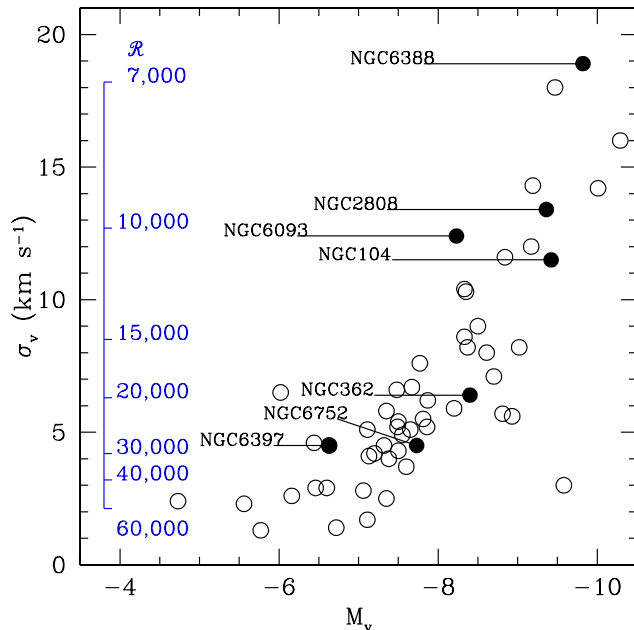


Figure 1. The distribution of Galactic GCs in absolute magnitude vs. line-of-sight velocity dispersion (Pryor & Meylan 1993). The inset scale shows the limiting line-width (and thus spectral resolution, $R = \lambda/\Delta\lambda$) obtainable for GCs as a function of the line-of-sight velocity dispersion, σ_v .

relative to $[\text{Fe}/\text{H}]$ is therefore a rough constraint on the star formation rate. Comparison with overall abundance then constrains the timescale of formation.

Unfortunately, the Milky Way is currently the only galaxy for which even a partial history of formation and enrichment can be traced in the stellar fossil record through to the present day. This is because detailed abundance analysis requires high signal-to-noise ratios and high spectral resolutions ($S/N \geq 60$, $R > 20,000$). Old stars are too faint to be studied in this way beyond the nearest dwarf spheroidal members of the Local Group (≤ 100 kpc). Even in the nearest gas-rich irregulars of the Local Group, abundance measurements are limited to a few very luminous supergiants (*e.g.* Venn *et al.* 2004), and results can only be obtained for a few elements. Moreover, these bright supergiants are very massive (young) and so only identify the recent gas composition. The history of a galaxy can only be learned from long-lived, low-mass stars, which are too faint for high-resolution spectroscopy beyond the nearest dwarf spheroidal galaxies (*e.g.* Shetrone *et al.* 2003).

These limitations drive us to target Globular clusters (GCs). Unlike single stars, high-resolution spectra *can* be obtained of unresolved GCs out to ~ 4 Mpc with *current* telescopes. GCs are bright enough ($-10 < M_v < -6$ mag) and have low enough velocity dispersions ($2 - 20$ km/s) that even weak lines (~ 15 mÅ) could be detected in spectra of their integrated light. Moreover, several lines of evidence from photometry and low-resolution spectroscopy already suggest

that GCs trace the star formation and the global formation history of their parent galaxy: the number of GCs per galaxy is roughly constant relative to the total light and mass of a galaxy; young GCs are found in regions of active star formation (*e.g.* Schweizer & Seitzer 1993, Barth *et al.* 1995); and the properties of both metal-rich (red) and now also metal-poor (blue) GC systems seem to correlate with the properties of their parent galaxies (*e.g.* Zepf & Ashman 1993, Geisler, Lee & Kim 1996; Gebhardt & Kissler-Patig 1999; Kundu & Whitmore 2001; Larsen *et al.* 2001; Strader, Brodie, & Forbes 2004). All of which implies that GCs are bright, observable markers of the chemical enrichment record of normal galaxies.

Of course, significant progress has also been made in understanding the chemical enrichment histories of elliptical galaxies and bulges from analysis of low-resolution, integrated-light (IL) spectra using line indexes, such as the Lick system (Burstein *et al.* 1984, Faber *et al.* 1985, Worthey *et al.* 1994, Worthey & Ottaviani 1997, Trager *et al.* 1998). These indexes provide estimates of age and composite “metallicity” (“Z”) based on lines from multiple elements such as Fe, Mg, and Ca (see Rose 1984, Worthey *et al.* 1994, and Worthey & Ottaviani 1997). GCs are ideal targets for these index systems as they are nearly ideal, single-age stellar populations.

A great deal of progress has recently been made with line index systems by using various kinds of principle component analysis to obtain better leverage on Z and also to obtain an “E” parameter, which includes all of the elements (O, Mg, C, etc) typically found to be enhanced in elliptical and bulge (rapidly forming) populations (Proctor & Sansom 2002; Proctor, Forbes, Beasley 2004; Strader & Brodie 2004). However, even for GCs, information from line indexes are limited by two difficulties. First, E and Z do not have the interpretive power of detailed abundances because they include elements which form in multiple sites and include elements which are known to be affected by GC self-enrichment (see discussions in Gratton, Sneden & Carretta 2004). These indexes do not entirely isolate the $[\alpha/\text{Fe}]$ ratios which constrain formation timescales. Second, line index results are very sensitive to the calibration of the system, and it can be hard to obtain stellar libraries of the appropriate age and enrichment or to know what calibration to use. This complication has been widely discussed in the literature (*e.g.* Trippico & Bell 1995; Trager *et al.* 2000ab; Thomas, Maraston, & Bender 2003; Proctor *et al.* 2004; Tantaló & Chiosi 2004). Adjustments to the calibration system have been published recently based on stellar models which include a range of enrichments. However, not all of these agree with each other and the models themselves are not well tested against observed populations. This concern is particularly relevant given recent work on M31, which shows that the Milky Way GC system may not be generally representative of GCs in even spiral galaxies; M31 appears to contain a disk GC system (Morrison *et al.* 2004) which is at least partly composed of young GCs (0.1–0.8 Gyrs; Barmby *et al.* 2000, Beasley *et al.* 2004) with different abundance patterns than are seen in the Milky Way (Burstein *et al.* 2004).

Fortunately, it *is* possible to obtain high-resolution spectra of unresolved GC. A typical GC has velocity dispersions of $2 < \sigma_v < 20$ km/s (Pryor & Meylan 1993, see Figure 1), so that spectra of their integrated light can have line widths in the range $60,000 > \lambda/\Delta\lambda > 6,500$. For comparison, an elliptical has $\sigma_v \sim 200$

km/s or greater and limiting line widths of $\lambda/\Delta\lambda \sim 1500$. Absorption features as weak as a ~ 15 mÅ can therefore be seen in high-resolution, *integrated light* spectra of all but the most massive GCs with $S/N \approx 60 - 90$.

Detailed abundances have never been obtained for unresolved GCs because current methods of abundance analysis only work for individual stars. We describe here progress that we have made in adapting the basic techniques of single star abundance analysis to spectra of integrated-light.

2. A Method for Light-Weighted Abundance Analysis

Abundances are not directly observable quantities; the strength of any given absorption line is a function not only of the abundance of the element, but also of the physical properties (e.g. mass and temperature) of the star. The method we are developing for analyzing IL spectra is based on the standard techniques used to analyze individual stars.

The standard technique for abundance analysis of single stars involves comparing the observed equivalent widths (EWs) of lines for each species with those predicted by model stellar atmospheres and spectral line synthesis. The model atmospheres have the following, observationally constrained parameters: effective temperature (T_{eff} , from $B - V$), specific gravity ($\log g$, from luminosity), and microturbulence (ξ). In principle, the only free parameter is abundance, $[A/H]$. So far, we have used Kurucz models in which Fe alone is varied, so that $[A/H]$ is roughly $[\text{Fe}/H]$. The Kurucz model atmosphere grids (available from R. Kurucz at <http://cfaku5.harvard.edu>) give optical depth, temperature, pressure, and electron density in each of 64 layers. The EW of any particular spectral line is then found by radiative transfer through these layers. Given the model atmosphere, the EW of a line is uniquely determined by the wavelength (λ), excitation potential (EP), and gf value of the line, and by the abundance of the element in question, $[X/H]$. Of these, only $[X/H]$ is adjusted. In standard analysis, the best model atmosphere is found by adjusting $[\text{Fe}/H]$ in the line synthesis and model atmospheres until a unique, self-consistent solution is found from all Fe I and Fe II lines (~ 100 lines). A strong constraint on the correct model atmosphere comes from requiring that Fe I lines over the full range of λ , EP, and EW give a stable Fe solution. This requirement is used to adjust T_{eff} , $\log g$, and ξ to find the appropriate stellar atmosphere model. Lines from any other element are then uniquely determined by the input abundance of that element ($[X/H]$) in the line synthesis step. The right abundance is found by adjusting this value until predicted EWs match those observed.

To interpret an IL spectrum, we have developed an original method of detailed chemical abundance analysis which involves producing a light-weighted EW, building on those techniques used for individual stars. For a *resolved* Galactic GC, the observed CMD tells us the exact fraction of light coming from every stellar type in the cluster. For NGC 6397, for instance, Figure 2 shows the CMD of NGC 6397 with boxes indicating groups of stars which each contain roughly 5% of the cluster's light. Based on this observed CMD, we can compute a model atmosphere for each box using the Kurucz model atmospheres (ATLAS9) for a range in abundance, $[A/H]$. We have developed code which then synthesizes the individual Fe lines by iteratively calling the spectrum synthesis program MOOG

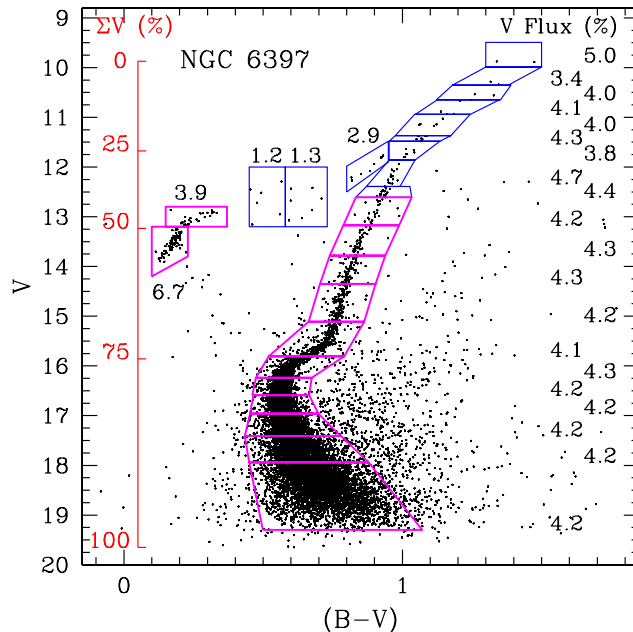


Figure 2. A color–magnitude diagram for NGC 6397 (Kaluzny 1997). The scale on the left shows the cumulative V -band flux coming from bright to faint stars. The boxes sub-divide the stellar population into groups containing $\sim 5\%$ of the V -band light, as indicated. An analysis based on this CMD, for example, would include one stellar atmosphere model per box.

(Snedden 1974) and varying the Fe in the line synthesis only until consistent solutions are obtained. With this Fe abundance, we can then compute a final stellar atmosphere for each box. We then identify the abundances of other elements by adjusting $[X/H]$ (in the line synthesis only) to match the observed EWs for a species. In this analysis, a microturbulence scaling law is adopted ($\xi \propto \log gf$).

As a first test of this basic strategy, we have analyzed the integrated light spectrum of NGC 6397 using its observed CMD (see Figure 2) to define the contributing stellar atmosphere models and their weights. From this analysis, we successfully obtain abundances for Fe–peak, α -elements, and light elements which are in good agreement with the results from other groups for single stars in NGC 6397 (see Bernstein & McWilliam 2001 and Bernstein & McWilliam 2005). However, when we target extragalactic GCs, we will not be able to use resolved CMDs to empirically identify the right mix of stellar populations. We must therefore learn to use theoretical CMDs — isochrones based on stellar evolution tracks — to analyze the IL spectra. To do this, and to understand the limitations and impact of stellar evolution models themselves, we have observed a set of GCs in the Milky Way and LMC to serve as a “training set”.

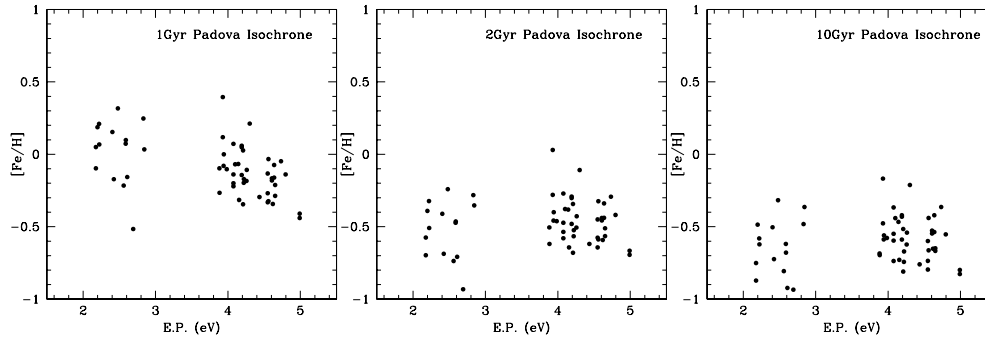


Figure 3. Excitation potential vs $[\text{Fe}/\text{H}]$ for all iron lines measured in the IL of 47 Tuc. Each plot shows the best-fit $[\text{Fe}/\text{H}]$ solution for one isochrone. A systematic negative trend is clear in the 1 Gyr isochrone, but weak in older isochrones. Scatter is largely due to uncertain gf values. It should be possible to obtain greater precision by using gf values tuned to the abundance solution of Arcturus, a nearby metallicity reference star. In RGB star analysis, such techniques reduce the scatter in EP vs. $[\text{Fe}/\text{H}]$ to ± 0.05 rms.

3. A Training Set of Galactic and LMC GCs

Our “training set” consists of seven Milky Way and eight LMC GCs. These span the range of velocity dispersions, abundances, ages, and HB morphologies available in the Milky Way and LMC systems (see Figure 1 and Table 1). For each of the training set GCs, we have obtained integrated light spectra by uniformly scanning the central 32×32 arcsec² and 12×12 arcsec² in the Milky Way and LMC GCs, respectively. Crucially, these clusters are all spatially resolved, so detailed color magnitude diagrams (CMDs) can provide age estimates and *a priori* knowledge of the member stellar populations, including HB morphology. We can use this information to refine our methods and determine how such variables affect our results. Moreover, we can also identify individual red giant branch (RGB) stars from these CMDs and use spectra of these individual stars to obtain “fiducial” abundances by standard methods which are consistent with our own atmospheric modeling and synthesis for the integrated light. Below we describe the results we have obtained for one Milky Way GC: NGC 104 (47 Tuc).

To analyze 47 Tuc as we would an unresolved GC, we use isochrones as the template for its stellar population. The analysis here uses isochrones based on the stellar evolution tracks of the Padova group (Girardi *et al.* 2000) and a Kroupa IMF (Kroupa & Boily 2002). We complete the same analysis for isochrones with a range of age and abundance ($1\text{--}16$ Gyrs, $-2.3 < [\text{Fe}/\text{H}] < 0.2$). The first question one might ask is whether the resulting ~ 15 Gyr, $[\text{Fe}/\text{H}] \sim -0.7$ isochrone *looks* like the observed CMD of 47 Tuc. Two differences are evident, although not unexpected (*e.g.* Bergbusch & Vandenberg 2001): the isochrones include lower mass stars than are observed in the clusters and do not reproduce the observed AGB bump. The same problems exist with the BASTI (Pietrinferni *et al.* 2004) stellar evolution models. To begin, we use the Padova isochrones “as is,” with no adjustments for mass segregation or the AGB bump.

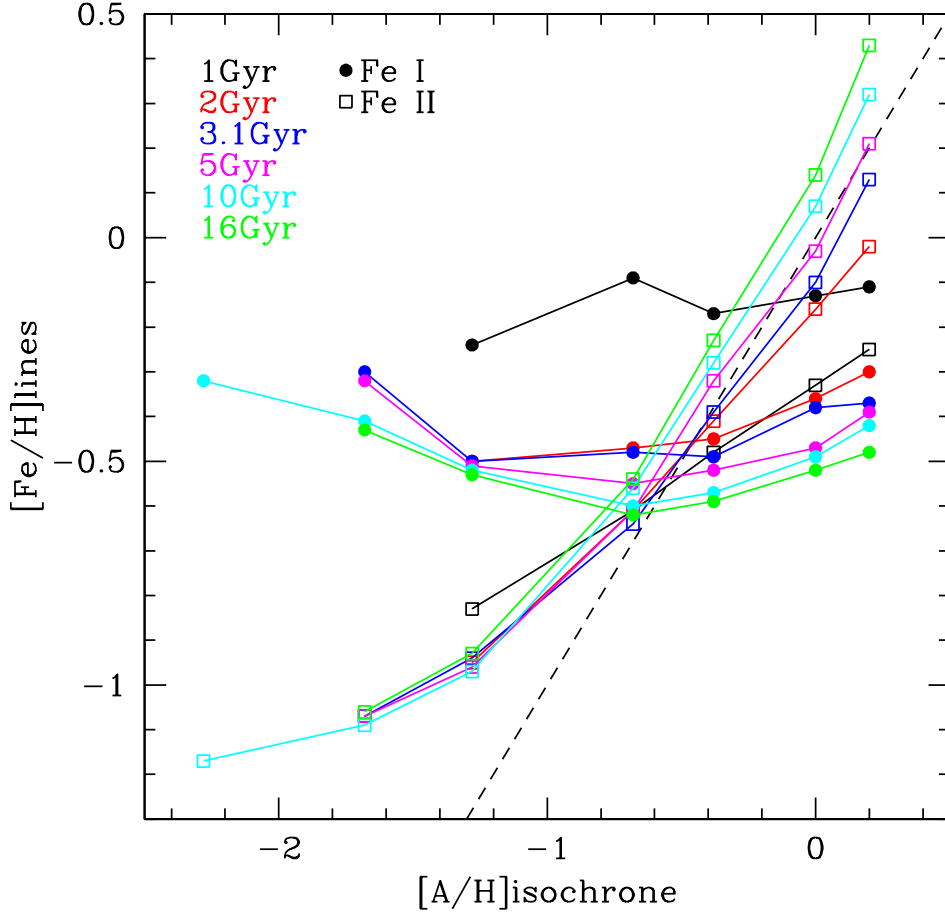


Figure 4. The inferred $[\text{Fe}/\text{H}]$ abundance from Fe I and Fe II lines for Padova isochrones of age 1–16 Gyrs and abundances of $[\text{A}/\text{H}] = -2.35$ to 0.2. These isochrones do not include α enhancement. The Fe I lines give stable solutions with λ and EP for isochrones with ages older than about 3 Gyrs (see Figure 3). The Fe II and Fe I lines give the same solution (the lines connecting Fe I and Fe II solutions cross) at a narrow range in abundances, namely at $[\text{Fe}/\text{H}] = -0.63 \pm 0.05$.

For each isochrone, we split the stellar population into roughly 20 groups each containing roughly 5% of the light, similar to the boxes shown in Figure 2. We then produce a stellar atmosphere for each group and synthesize a light-weighted EW for about 70 Fe I and 10 Fe II lines by combining the synthesized EWs from MOOG for each group, as described in §2. Note that with the isochrones, the parameters of the atmosphere model are completely dictated by the parameters of the isochrone. We adjust only the abundance of Fe in the line synthesis step to obtain a good match between observed and predicted EWs for

all Fe I and Fe II line. Figure 3 shows the best-match Fe value for Fe I lines as a function of excitation potential for three different isochrones. The average of these solutions gives us the inferred $[\text{Fe}/\text{H}]$ value (and a statistical uncertainty) for each isochrone. Preferred solutions have small *rms* scatter and no slope with excitation potential, wavelength, and EW. We then do the same test for Fe II lines. A plot showing the inferred value of $[\text{Fe}/\text{H}]$ from Fe I and Fe II lines for each isochrone is shown in Figure 4. Surprisingly, we find that best-fit $[\text{Fe}/\text{H}]$ solution from Fe I lines is nearly independent of the input isochrone *metallicity*, while Fe II lines are nearly independent of the input *age*. Together, the Fe I and Fe II lines provide an excellent constraint on the abundance of the cluster and a way to break the age-metallicity degeneracy that will never be achievable at low resolution.

From the best-fit isochrone, we get $[\text{Fe}/\text{H}] = -0.63 \pm 0.03$ (1σ statistical uncertainty). We then adjust the luminosity function of one isochrone to remove low-mass stars and add an AGB bump. With this adjusted isochrone, we find $[\text{Fe}/\text{H}] = -0.73$. Note that these results differ by only 0.1 dex, and that both results are roughly within the range of values obtained recently by different groups from individual stars (Kraft & Ivans 2003, Carretta *et al.* 2004). Nevertheless, the change in our $[\text{Fe}/\text{H}]$ solution with these adjustments emphasizes the importance of the luminosity function to our results. We will use the rest of the training set to determine the best approach to dealing with these differences between isochrones and real CMDs.

We use the adjusted isochrone to then obtain abundances for a broad range of key elements (see Table 2). Our final abundances are in good agreement with those in the literature for individual 47 Tuc stars. Moreover, we find the expected abundance patterns α - (enriched relative to solar), Fe-peak (roughly solar), and r-process (enriched) elements that one would expect for an old globular cluster. We also detect enrichment of Na and Al, which is consistent with self-enrichment through proton-burning in AGB stars and is found for some individual stars (with star-to-star variations) in 47 Tuc (Carretta *et al.* 2004). This suggests that we will be able to measure such abundance variations in unresolved clusters even if present in only a fraction of the stars in a given cluster! Finally, we note that the age of 47 Tuc is only constrained from our analysis to be greater than ~ 3 Gyrs. We may be able to improve this by calibrating the $\log gf$ values of individual Fe lines to the abundance solution for Arcturus; doing so should reduce the scatter in plots like those shown in Figure 3 to ± 0.05 , as it does in the analysis of individual stars (see Bernstein & McWilliam 2005). However, it is also clear from evolutionary tracks and observed CMDs of Milky Way GCs that stellar populations themselves simply do not vary much with age after a few Gyrs (*e.g.* Yi *et al.* 2003).

4. Further Spectroscopic Constraints on Integrated Light Abundances

An important issue to explore is the influence of Horizontal Branch (HB) morphology on our abundance analysis because it is not uniquely correlated with age or metallicity and therefore not reliably characterized by the isochrones. Balmer line EWs *and profiles* will be helpful in this regard, because they are very sensitive to the light fraction contributed by hot stars (*e.g.* Bernstein & McWilliam

2002; Schiavon *et al.* 2004; Bernstein & McWilliam 2005;). To this end, we have compared observed Balmer profiles for several of our training set clusters with synthesized, light-weighted Balmer profiles based on the isochrones. Our preliminary work suggests that we will need to also synthesize blended lines in the Balmer line wings in order to get accurate Balmer EWs and profiles, particularly in the metal rich clusters. This may be a particular problem for low-resolution spectra. Similar issues have already been noted in the literature to the extent that Balmer line indexes in low-resolution spectra seem to be sensitive to the calibration of the line system (*e.g.* Proctor, Forbes & Beasley 2004). Additional constraints may also come from CaII lines, which have also been shown to track HB color in low-resolution spectra (*e.g.* Burstein *et al.* 2004; Proctor, Forbes & Beasley 2004). Independent models for horizontal branch morphology can also be combined with the isochrone models directly to explore the impact on inferred abundances

We are also planning to explore a broader range of parameters in the isochrones themselves as more models become publicly available. For example, stellar evolution tracks with different abundance ratios (*e.g.* enriched in α -elements or with different helium fractions) may yield systematically different abundances and should also be tested against the training set.

5. Applications

It is already possible to obtain spectra of extragalactic GCs that can be analyzed with this technique. In the local group, abundances of the more distant LMC GCs could be obtained in a few hours with 4-m class telescopes taking IL spectra, instead of requiring many hours of exposure time on 8-m class telescopes observing individual cluster stars. Beyond the LMC, a handful of galaxies within 4-5 Mpc can be observed using using current 6.5-10 m telescopes. We have already obtained a few spectra ($R \sim 20,000$, S/N= 60 - 900 at $H\alpha$) of confirmed GCs in galaxies NGC 1313 and NGC 5128 (both ~ 4 Mpc away) with the MIKE echelle spectrograph (Bernstein *et al.* 2003) on the Magellan Telescopes. In the future, hundreds of galaxies in the local universe could be observed with the next generation of ground-based 20-30 m telescopes. In addition, the abundances and integrated light spectra we already have in hand can be used to better understand and calibrate the low-resolution data and line-index systems. This is important because line indexes will always be able to reach galaxies at greater distances than the high-resolution technique described here.

Acknowledgments. We gratefully acknowledge the help of Las Campanas technical staff and particularly telescope operators Fernando Peralta and Herman Olivares. R. A. B. acknowledges partial support from NASA through Hubble Fellowship grant HF-01088.01-97A awarded by Space Telescope Science Institute, which is operated for NASA by the Association of Universities for Research in Astronomy, Inc. under contract NAS 5-2655. A. M. acknowledges support from NSF grants AST-96-18623 and AST-00-98612. We also thank the organizers for a very enjoyable and stimulating conference.

Table 1. “Training set” clusters in the Milky Way and LMC.

GC	RA (J2000)	Dec (J2000)	μ_V mag/asec ²	V_{tot} mag	$M_{V_{\text{tot}}}$ mag	HBR ^a	R_{\odot} kpc	r_{core}^b pc	$\sigma_{v\text{core}}$ km/s	[Fe/H]
Milky Way clusters										
NGC 104	00 24 05.2	-72 04 51	14.42	3.95	-9.42	-0.99	4.5	0.40	9.8	-0.65
NGC 362	01 03 14.3	-70 50 54	14.79	6.40	-8.40	-0.87	8.5	0.17c	6.3	-1.16
NGC 2808	09 12 02.6	-64 51 47	15.17	6.20	-9.39	-0.49	9.6	0.26	14.2	-1.15
NGC 6093	16 17 02.5	-22 58 30	15.38	7.33	-8.23	0.93	10.0	0.15	12.5	-1.75
NGC 6388	17 36 17.0	-44 44 06	14.50	6.72	-9.82		11.5	0.12	18.9	-0.60
NGC 6397	17 40 41.3	-53 40 25	16.66	5.73	-6.63	0.98	2.3	0.05c	3.3	-1.95
NGC 6752	19 10 51.8	-59 58 55	15.20	5.4	-7.73	1.00	4.0	0.17c	4.5	-1.83
LMC clusters										
log(Age)										
Old (> 5Gyrs)										
NGC 1916	5 18 39.00	-69 24 24	15.8	9.88	-8.96		>9	< 1.5	8.2 ± 1.2	-2.08
NGC 2019	5 31 56.7	-60 09 33	15.5	10.7	-7.94		>9	0.9	7.5 ± 1.3	-1.3
NGC 2005	5 30 10.36	-69 45 09	15.8	11.57	-7.48		>9	1.3	8.1 ± 1.3	-1.92
Intermediate age (0.1–1.5G yrs)										
NGC 1866	5 13 39	-65 27 54	18.5	9.76	-8.74		8.1	11.7	...	-0.51
NGC 1978	5 28 45.00	-66 14 12		10.7	-7.7		9.3	...	3.0 ± 0.5	-0.91
Young (~ 10 Myr)										
NGC 1711	4 50 37	-69 59 06	17.0	10.11	-8.3		7.4	5.7	...	-0.6
NGC 2002	5 30 21	-66 53 00	16.0	10.1	-8.3		7.2	3.5
NGC 2100	5 42 08	-69 12 42	17.0	9.6	-8.8		7.2	6.7

Notes: (a) HBR, the horizontal-branch ratio, is defined as $(B - R)/(B + V + R)$. (b) A “c” indicates that the cluster is core-collapsed. For the Milky Way GCs, values for 1-D velocity dispersion, σ_v , are from Pryor & Meylan (1993); all other values are from Harris (1996). Data for the LMC clusters comes from various sources, including Johnson *et al.* 2004, Hill (2004), Olsen *et al.* 1998, Olszewski *et al.* 1996 and references therein.

Table 2. Element Abundances for 47 Tuc from Integrated Light Spectra

Species, X	$\epsilon(X)^a$	σ	N_{lines}	$(\sigma/\sqrt{N})^b$	$[X/\text{Fe}]^c$	$[X/\text{Fe}]^d$
<u>Fe-peak</u>						
Sc II	2.53	...	1	...	+0.13	+0.13
V I	3.40	0.31	5	0.16	+0.11	+0.05
Cr I	4.87	0.14	3	0.10	-0.19	+0.11
Mn I	4.49	0.30	4	0.17	-0.31	-0.29
Fe I	6.78	0.24	71	0.03	-0.73	-0.67, -0.63 ^f
Fe II	6.81	0.15	8	0.06	-0.70	-0.56, -0.58 ^f
Ni I	5.47	0.18	12	0.05	-0.05	+0.06
<u>α-elements</u>						
Si I	7.16	0.21	6	0.09	+0.33	+0.30
Ca I	5.81	0.24	12	0.07	+0.19	+0.20
Ti I ^g	4.55	0.24	13	0.07	+0.34	+0.26
Ti II ^g	4.68	0.16	3	0.11	+0.44	+0.38
<u>Light elements with possible intra-cluster variations</u>						
Mg I	7.02	...	1	...	+0.17	+0.40
Al I	6.19	0.02	2	0.02	+0.43	NA
<u>Neutron-capture elements (s-, r-process)</u>						
Y II	1.34	...	1	...	-0.19	+0.49 ^e
Y I:	1.29	...	1	...	-0.24	NA
Zr I	1.80	0.21	2	0.21	-0.08	-0.22 ^e
Ba II	1.41	0.09	3	0.05	-0.11	NA
La II	0.57	0.38	2	0.26	+0.05	NA
Nd II	0.80	...	1	...	+0.01	NA
Eu II	-0.12	...	1	...	+0.04	+0.36 ^e

Notes: (a) The abundance of element X is defined as $\epsilon(X) = \log_{10}[\text{N}(X)/\text{N}(\text{H})] + 12$. (b) Realistic uncertainties probably lie between the *rms* error, σ , and the error in the mean, σ/\sqrt{N} . (c) $[X/\text{Fe}] = \epsilon(X/\text{Fe}) - \epsilon(X/\text{Fe})_{\odot}$. For Fe I and Fe II this column indicates $[\text{Fe}/\text{H}]$. (d) From Carretta *et al.* (2004). (e) From Brown & Wallerstein (1989). (f) From Kraft & Ivans (2003) using the Kurucz models; also, values of -0.70 and -0.65 were obtained from Fe I and Fe II, respectively, using the Gustafsson *et al.* (1975) models. (g) Ti can also be considered an Fe-peak element and does show different abundance ratios than Si in Galactic GCs (Lee & Carney 2002).

References

- Ashman, K.M. & Zepf, S.E. 1993, MNRAS, 264, 611
 Barmby, P., Huchra, J.P., Brodie, J.P., Forbes, D.A., Schroder, L.L., & Grillmair, C.J. 2000, AJ, 119, 727
 Barth, A.J., Ho, L.C., Filippenko, A.V., & Sargent, W.L.W. 1995, AJ, 110, 1009
 Beasley, M.A., Brodie, J.P., Strader, J., Forbes, D.A., Proctor, R.N., Barmby, P., Huchra, J.P. 2004, AJ, 129, 1412
 Bensby, T., Feltzing, S., & Lundstrom, I. 2004a, A&A, 415, 155
 Bensby, T., Feltzing, S., & Lundstrom, I. 2004b, A&A, 421, 969

- Bergbusch, P.A. & Vandenberg, D.A. 2001, *ApJ*, 556, 322
- Bernstein, R.A. & McWilliam, A. 2002, *Extragalactic Star Clusters*, IAU Symposium #207, eds. A. Grebel, D. Geisler, D. Minniti, (San Francisco: ASP), 739
- Bernstein, R. A., Shtetman, S. A. Gunnels, S. M., Mochmacki, S. & Athey, A. E. 2003, *SPIE*, 4841, 1694
- Bernstein, R. A. & McWilliam, A. 2005, in prep.
- Burstein, D., Faber, S.M., Gaskell, C.M., Krumm, N. 1984, *ApJ*, 287, 586
- Burstein, D. Li, Y. *et al.* 2004, *ApJ*, 614, 158
- Carretta, E. & Gratton, R.G., Bragaglia, A., Bonifacio, P. & Pasquini, L. 2004, *A&A*, 416, 925
- Edvardsson, B., Andersen, J., Gustafsson, B., Lambert, D.L., Nissen, P.E., Tomkin, J. 1993, *A&A*, 275, 101
- Faber, S.M., Friel, E.D., Burstein, D., Gaskell, C.M. 1985, *ApJS*, 57, 711
- Fulbright, J., McWilliam, A., & Rich, R.M. 2005, *ApJ*, submitted
- Gebhardt, K. & Kissler-Patig, M. 1999, *AJ* 118, 1526
- Geisler D., Lee M. G., Kim E., 1996, *AJ*, 111, 1529
- Girardi, L., Bressan, A., Bertelli, G., Chiosi, C. 2000, *A&AS*, 141, 371
- Gratton, R., Sneden, c., Carretta, E. 2004, *ARA&A*, 42, 385
- Gustafsson, B., Bell, R. A., Ericksson, K., & Nordlund, A. 1975, *A&A*, 42, 407
- Hill, V. 2004, in *Carnegie Obs. Astrophysics Series, Vol. 4: Origin and Evolution of the Elements*, ed. A. McWilliam and M. Rauch (Pasadena: Carnegie Obs.), (<http://www.ociw.edu/ociw/symposia/series/symposium4/proceedings.html>)
- Johnson, J.A., Bolte, M., Hesser, J.E., Ivans, I.I., and Stetson, P.B. 2004, in *Carnegie Obs. Astrophysics Series, Vol. 4: Origin and Evolution of the Elements*, ed. A. McWilliam and M. Rauch (Pasadena: Carnegie Obs.), (<http://www.ociw.edu/ociw/symposia/series/symposium4/proceedings.html>)
- Kaluzny, J. 1997, *A&AS*, 112, 1
- Kraft, R.P. & Ivans, I.I. 2003, *PASP*, 115, 143
- Kroupa, P. & Boily, C. M. 2002, *MNRAS*, 336, 1188
- Kundu A. & Whitmore B. C. 2001, *AJ*, 121, 2950
- Larsen S. S., Brodie J. P., Huchra J. P., Forbes D. A., Grillmair C. J., 2001, *AJ*, 121, 2974
- Lee, J.-W. & Carney, B.W. 2002, *AJ*, 124, 1511
- McWilliam, A., Preston, G.W., Sneden, C., Searle, L. 1995, *AJ*, 109, 2757
- Morrison, H.L, Harding, P., Perrett, K., Hurley-Keller, D. 2004, *ApJ*, 603, 87
- Olsen, K.A.G., Hodge, P.W., Mateo, M. *et al.* 1998, *MNRAS*, 300, 665
- Olzewski, E.W., Suntzeff, N.B., Mateo, M., 1996, *ARA&A*, 34, 511
- Pietrinferni A., Cassisi S., Salaris M. & Castelli F. 2004, *ApJ*, 612, 168
- Prochaska, J. X., Naumov, S. O., Carney, B. W., McWilliam, A., & Wolfe, A. M. 2000, *ApJ*, 120, 2513
- Proctor, R.N. & Sansom, A.E. 2002, *MNRAS*, 333, 517
- Proctor, R.N., Forbes, D.A., Hau, G.K.T., Measley, M.A., de Silva G.M., Contreras, R., Terlevich, A.I. 2004, *MNRAS*, 349, 1381
- Proctor, R.N., Forbes, D.A. & Beasley, M.A. 2004, *MNRAS*, 335, 1327
- Pryor, C. & Meylan, G. 1993, in *Structure and Dynamics of Globular Clusters*, ASP Conf. Ser. Vol. 50, Eds. S.G. Djorgovski and G. Meylan, (San Fransisco: ASP), 357
- Rose, J.A. 1984, *AJ*, 89, 1258
- Schiavon R.P., Rose J.A., Courteau S., MacArthur L.A., 2004, *ApJ*, 608, L33
- Schweizer, F. & Seitzer, P. 1993, *ApJ*, 417, L29
- Shetrone, M., Venn, K. A., Tolstoy, E., *et al.* 2003, *AJ*, 125, 684
- Sneden, C. 1974, *ApJ*, 189, 493
- Strader, J., Brodie, J.P. & Forbes, D.A. 2004, *AJ*, 127, 3431
- Strader, J., Brodie, J.P. 2004, *AJ*, 128, 1671
- Tantalo, R. & Chiosi, C. 2004, *MNRAS*, 353, 917

- Thomas, D., Maraston, C., Bender, R. 2003 MNRAS, 339, 897
Trager, S.C., Worthey, G., Faber, S.M., Burstein, D., Gonzalez, J.J. 1998, ApJS, 116, 1
Trager, S.C., Faber, S.M., Worthey, G., Gonzalez, J.J. 2000a, AJ, 119, 1645.
Trager, S.C., Faber, S.M., Worthey, G., Gonzalez, J.J. 2000b, AJ, 120, 165.
Tripicco, M.J. & Bell, R.A. 1995, AJ, 110, 3035
Venn, K., *et al.* 2004, in Carnegie Obs. Astrophysics Series, Vol. 4: Origin and Evolution of the Elements, ed. A. McWilliam and M. Rauch (Pasadena: Carnegie Observatories,
<http://www.ociw.edu/ociw/symposia/series/symposium4/proceedings.html>)
Worthey, G. 1994, ApJS, 95, 107
Worthey, G. & Ottaviani, D.L. 1997, ApJS, 111, 377
Yi, S. K., Kim, Y., & Demarque, P. 2003, ApJS, 144, 259
Zepf, S.E. & Ashman, K.M., 1993, MNRAS, 264, 611